

Proton dynamics in supercritical water

C. Andreani

Università degli Studi di Roma Tor Vergata, Dip.to di Fisica and Istituto Nazionale per la Fisica della Materia, UdR Tor Vergata, via della Ricerca Scientifica 1, 00133, Rome, Italy

D. Colognesi

Consiglio Nazionale delle Ricerche, Gruppo Nazionale Struttura della Materia, viale dell'Università 11, 00185 Roma, Italy

E. Degiorgi^{a)} and M. A. Ricci

Università degli Studi Roma Tre, Dip.to di Fisica "E. Amaldi" and Istituto Nazionale per la Fisica della Materia, UdR Roma Tre, via della Vasca Navale 84, 00146, Rome, Italy

(Received 17 May 2001; accepted 1 October 2001)

An inelastic neutron scattering experiment has been performed on supercritical water at high momentum transfer, up to 90 \AA^{-1} , in order to study single proton dynamics. The value of the proton mean kinetic energy has been extracted in the framework of the impulse approximation. The anisotropy of the proton momentum distribution inside a single water molecule is discussed. The extracted experimental mean kinetic energy is found in good agreement with the predictions of a harmonic model, under the assumptions of decoupling between translational, rotational and vibrational degrees of freedom. Differences emerge between our results and those obtained in a recent inelastic neutron scattering experiment on water in sub- and supercritical conditions. These differences are pointed out and examined in detail. © 2001 American Institute of Physics.

[DOI: 10.1063/1.1420751]

I. INTRODUCTION

The properties of supercritical water and aqueous solutions have implications in many different fields of research and industry and are very different from those found under normal temperature and pressure conditions. It has been argued through neutron diffraction studies¹ that the strong modifications undergone by the hydrogen bond network when the sub- and supercritical conditions are approached may be responsible for such large differences. These studies have stimulated an increased interest as regards the dynamical properties of water in these thermodynamic conditions.^{2–4} In this paper we present a determination of the proton mean kinetic energy, $\langle(E_K)_H\rangle$, in supercritical water by using the Deep Inelastic Neutron Scattering (DINS) technique. Aims of this study are twofold. The first one is to test the validity of the harmonic approximation and of the hypothesis of decoupling among translational, rotational and vibrational degrees of freedom in supercritical water. Due to the substantial disruption of the H-bond network in the supercritical regime,¹ indeed we expect that the different degrees of freedom of a water molecule can be treated as decoupled. The second aim is to assess the anisotropy of the proton momentum distribution due to the nonspherical molecular symmetry in water as already evidenced in H_2S .⁵

In a recent paper a DINS experiment has been reported on water in sub- and supercritical conditions and the proton mean kinetic energy, $\langle(E_K)_H\rangle$, extracted.⁶ The experimental $\langle(E_K)_H\rangle$ values have been compared with theoretical predictions within the harmonic approximation and decoupling

hypothesis.⁶ Surprisingly the theoretical predictions reported therein severely underestimate the experimental data in supercritical conditions, while better agreement, between theory and experiment, is found at lower temperatures. As a matter of fact in the latter thermodynamical condition one would expect the decoupling of degrees of freedom not to hold anymore.⁷ These anomalous findings represent an additional reason for further investigations of water proton dynamics in supercritical conditions.

In Sec. II we report the details of experiment and data analysis; in Sec. III the model calculation is introduced and the comparison between the isotropic and anisotropic proton momentum distributions is presented. The results are finally discussed in Sec. IV.

II. EXPERIMENT AND DATA ANALYSIS

The experimental measurements have been performed at the inverse-geometry electron-volt spectrometer eVS, operating at the ISIS pulsed neutron source (Rutherford Appleton Laboratory, Chilton, Didcot, UK), using an incident pulsed neutron beam in the energy range (5–70) eV.⁸ The scattered neutron energies have been determined by a resonance filter difference technique.⁹ In this technique, four ^{197}Au filters, mounted on aluminum frames, are placed between the sample and detectors and cycled in and out of the scattered neutron beam every 300 s, in order to average out the possible drifts in detector efficiency during a single run. The difference between filter-in and filter-out measurements provides the number of neutrons absorbed by the foil and the energy of the scattered neutrons through the standard time-of-flight technique.⁹ The energy, E_0 , of the resonance of the

^{a)}Electronic mail: degiorgi@fis.uniroma3.it

10 μm thick ^{197}Au foil and the corresponding Full Width at Half Maximum (FWHM), ΔE_0 , were calibrated by measuring the scattering from a Pb sample at room temperature, yielding $E_0 = 4908(1)$ meV and $\Delta E_0 = 140(1)$ meV. These values agree with those reported in the literature.¹⁰

Measurements on supercritical water were performed on a high purity sample contained in a flat Ti–Zr alloy can with five internal cylindrical holes, 1.5 mm diameter each, 50 mm long. A single thermodynamic point has been investigated, corresponding to $T = 673.1(1)$ K, $p = 360(5)$ bar and $\rho = 0.483(5)$ g/cm³. The sample temperature was controlled with an accuracy of ± 0.1 K, using the standard ISIS sample environment equipment with heaters and two thermocouple sensors at the top and bottom of the sample container.

Neutron scattering spectra were recorded in the scattering angular range $28^\circ < 2\theta < 61^\circ$, using 24 ^6Li glass scintillator detectors placed at a distance of approximately 0.7 m from the sample, providing a corresponding momentum transfer at the maximum of the proton recoil peak, \bar{q} , in the range (26–90) \AA^{-1} .

The resolution function of a resonance inverse geometry instrument, such as eVS, has been described in detail in previous papers.^{8,11,12} This function is generally obtained from a convolution of geometrical and energy components, and determined through calibration measurements from a reference lead sample.⁸ The geometrical component, dominated by the angular uncertainty, is well described by a Gaussian function,¹¹ while the energy component, generated by the uncertainty associated with the value of the neutron absorption energy in the foil, can be represented by a Voigt function.¹⁰ Both contributions are angular dependent.

The difference between filter-in and filter-out spectra, after normalization to the monitor counts and detector efficiency, yielded the experimental Deep Inelastic Neutron Scattering (DINS) time-of-flight profiles.^{8,13} An example of these spectra for eight detectors is shown in Fig. 1. From this figure one can appreciate the change of the hydrogen recoil peak position as a function of the scattering angle with respect to the very intense peak resulting from the combined scattering of all the remaining masses (Ti, Zr and O). It is evident that, at smaller angles, the two peaks become very close to each other and they even begin to overlap. Therefore, in order to avoid possible distortions of the H peak lineshape (and the consequent introduction of systematic errors in the peak width evaluation), an accurate subtraction of the *nonhydrogenous* contribution has been performed. The empty container has been subtracted for each detector individually checking for the spectra showing residual spurious satellite peaks. For these spectra a further subtraction was performed to get rid of such spurious peaks which could lead to an anomalously higher and angle dependent proton peak width. As pointed out above these systematic errors are to be ascribed to a residual sample container signal which gradually superimpose to the wings of the proton recoil peak as the scattering angle decreases. As a matter of fact these errors are not properly corrected when the eVS standard subtraction routines are used. On the contrary a set of fitted widths showing no appreciable dependence on the scattering angle is obtained (see Sec. III) when the aforementioned more accurate

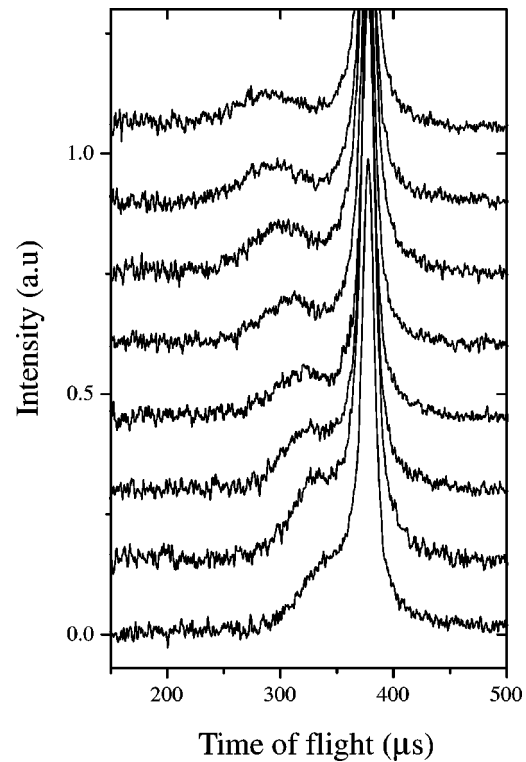


FIG. 1. Difference time-of-flight DINS neutron spectra from supercritical H_2O at $T = 673$ K, for eight detectors in the angular range $28.6^\circ < 2\theta < 43^\circ$ (bottom to top).

procedure is used. In this view we stress that the individual spectra analysis appears to be a necessary prerequisite in order to extract reliable $\langle (E_K)_H \rangle$ values from hydrogenous samples when they are contained in cells made with strong scattering materials.

A multiple scattering contribution from hydrogen in the spectra has also been estimated to be negligible by a Monte Carlo simulation routine.¹⁴

Data were subsequently analyzed, for each detector individually, in the DINS framework.^{15,16} This has been achieved in the usual way by coupling the energy transfer, $\hbar\omega$, and the momentum transfer, $\hbar q$, dynamic variables through the introduction of the scaling variable y .^{15,17}

$$y = \frac{M_H}{\hbar q} \left(\omega - \frac{\hbar q^2}{2M_H} \right), \quad (1)$$

and of the scaling response function, $F(y, q)$, defined as

$$F(y, q) = \frac{\hbar q}{M_H} S(q, \omega), \quad (2)$$

where $S(q, \omega)$ is the dynamic structure factor and M_H is the proton mass. We point out that within the Impulse Approximation (IA)^{15,18} the q dependence of the response scaling function can be dropped to yield

$$F(y) = \int d\vec{p} n_H(p) \delta \left(y - \frac{\vec{p} \cdot \hat{q}}{\hbar} \right), \quad (3)$$

where $n_H(p)$ is the momentum distribution of a single hydrogen nucleus in the molecular fluid. Thus, for an isotropic system, $F(y)$ is the distribution function of the proton mo-

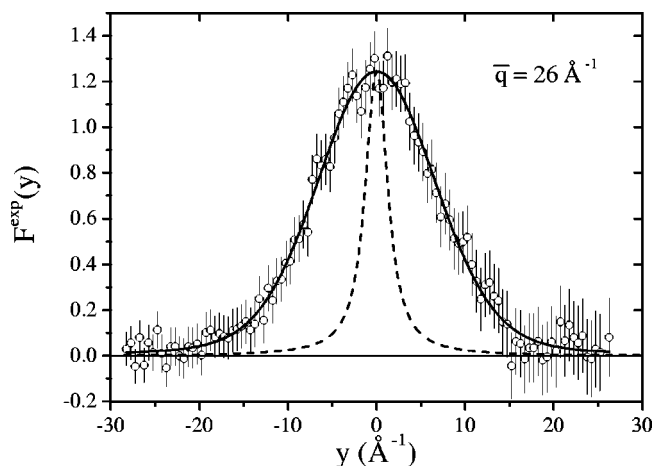


FIG. 2. Experimental (error bars) and fitted (full line) response functions, $F^{\text{exp}}(y)$, for supercritical water from DINS measurements for the scattering angle $2\theta=27.88^\circ$. A resolution contribution (dashed line) is also plotted.

mentum projected along the \hat{q} direction. The standard deviation of this distribution, σ_H , is linked to the hydrogen atom mean kinetic energy, $\langle(E_K)_H\rangle$, through the well-known relation:

$$\sigma_H^2 = \frac{2M_H}{3\hbar^2} \langle(E_K)_H\rangle. \quad (4)$$

In the present experiment the recoil energies of the “free” hydrogen atoms occur in the range (1.5–17) eV. Since the energy transfer is much higher than the largest vibrational energy quantum of the H_2O isolated molecule, i.e., 466 meV,⁴ the relation between the response function and the momentum distribution expressed by Eq. (3) can be reasonably assumed to hold in the whole scattering range. The experimental response function within the IA can then be expressed by

$$F_n^{\text{exp}}(y) = F(y) \otimes R_n(y), \quad (5)$$

where $R_n(y)$ is the experimental resolution for the n -th detector, in y -space. In Fig. 2 the experimental response function, $F_n^{\text{exp}}(y)$, for H_2O is shown for the scattering angle $2\theta = 27.88^\circ$. In this figure the resolution profile for the Au foil is also plotted.

III. RESULTS

In order to extract the single proton mean kinetic energy we assumed, as a first and temporary hypothesis, the $n_H(p)$ to be an isotropic Gaussian.^{5,19} Each detector spectrum has been fitted by a profile given by the convolution of a Gaussian, representing the function $F(y)$ [see Eq. (3)], with a Voigt function describing the instrument resolution [see Eq. (5)].¹⁶ A normalization factor was included as a free parameter. The fitting procedure, accomplished by a FORTRAN code, making use of the MINUIT minimization routine,²⁰ yielded a set of σ_H values, corresponding to different momentum transfers, i.e., to different scattering angles. The response function resulting from the fit at $2\theta=27.88^\circ$ is shown in Fig. 2 as an example.

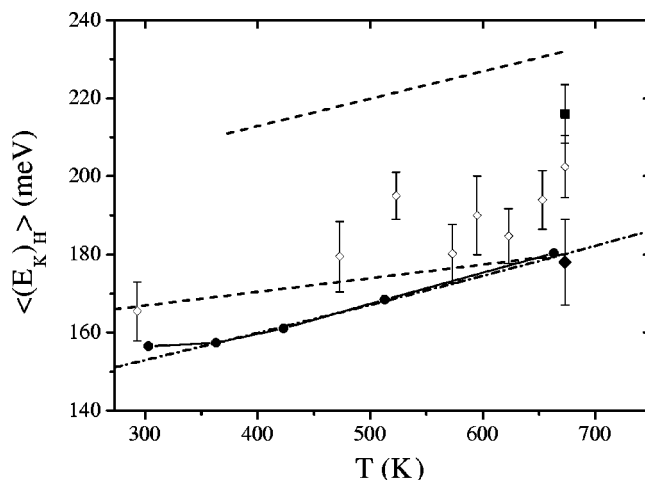


FIG. 3. Proton mean kinetic energy as a function of temperature. Values obtained from optical data are represented as a dot-dashed line for an isolated water molecule and as solid circles for the dense fluid along the coexistence curve and the supercritical state (the solid line is an eye guide). The open diamonds and the full squares are taken from Ref. 6 for supercritical water at constant density ($\rho=0.85\text{ g/cm}^3$) as a function of temperature, and at constant density ($\rho=0.52\text{ g/cm}^3$) and $T=673\text{ K}$, respectively. The result of the present experiment is reported as a full diamond. The dashed lines represent the proton mean kinetic energy values in diluted gas (upper) and dense supercritical water (lower) according to Ref. 6.

Values of σ_H for the different angles showed no q -dependence (see Sec. II), thus confirming the validity of the IA assumption for the present set of data and the reliability of the can subtraction procedure. The weighted mean of these quantities provides a value of $\langle\sigma_H\rangle=(5.3\pm0.2)\text{ \AA}^{-1}$ corresponding to a proton mean kinetic energy $\langle(E_K)_H\rangle=(178\pm11)\text{ meV}$ (see the full diamond in Fig. 3).

An independent determination of the quantity $\langle(E_K)_H\rangle$ can be obtained, following a procedure which has been described in detail in a previous paper on H_2S ,⁵ making use of spectroscopic data on supercritical H_2O .^{3,4} We remark that this procedure relies upon the harmonic approximation for all (internal and external) molecular normal modes. In this procedure the mean kinetic energy of a hydrogen nucleus belonging to a water molecule, neglecting the roto-vibrational interactions and any interplay between translational and internal motions, is written as the sum of three different contributions:

$$\langle(E_K)_H\rangle = \langle(E_K^{\text{tra}})_H\rangle + \langle(E_K^{\text{rot}})_H\rangle + \langle(E_K^{\text{vib}})_H\rangle, \quad (6)$$

where $\langle(E_K^{\text{rot}})_H\rangle$ and $\langle(E_K^{\text{tra}})_H\rangle$ are referred to as the external contributions to the kinetic energy and $\langle(E_K^{\text{vib}})_H\rangle$ is the internal vibrational contribution. By comparing the typical excitation frequencies derived from Raman spectroscopy,^{3,4} it appears that the mean kinetic energy is mainly determined by the internal molecular vibrations. In the following, the external contributions will be derived semi-classically, while for the internal mode contributions a full quantum description within the harmonic approximation will be retained.

(a) *Translational contribution.* It has been shown⁵ that starting from the classical expression for an isolated molecule:

$$\langle (E_K^{\text{tra}})_H \rangle = \frac{3}{2} \left(\frac{M_H}{M_T} \right) k_B T = 0.0839 k_B T, \quad (7)$$

an approximate evaluation of this quantity for a dense system can be obtained by introducing an *effective lattice temperature* T_{tra}^* . This can be calculated averaging all the N_p optical phonon frequencies, ω_λ , observed in Raman spectra:³

$$k_B T_{\text{tra}}^* \simeq \hbar \sum_{\lambda=1}^{N_p} \frac{\omega_\lambda}{2N_p} \coth \left(\frac{\hbar \omega_\lambda}{2k_B T} \right). \quad (8)$$

(b) *Rotational contribution.* The rotational (or librational) contribution to the mean kinetic energy for an isolated molecule can be classically expressed by

$$\begin{aligned} \langle (E_K^{\text{rot}})_H \rangle &= \left[1 + \left(\frac{M_O}{M_T} \right) + \left(\frac{\rho^2 + 1}{\rho^2 + M_T/M_O} \right) \right] \frac{1}{4} k_B T \\ &= 0.71 k_B T, \end{aligned} \quad (9)$$

where $\rho = (M_T/M_O) \tan(\alpha/2)$ and α is the H–O–H angle, equal to 104.5°. As for the translational contribution an *effective rotational–librational temperature*, T_{rot}^* , can be introduced⁵ for a dense sample, averaging all the N_l observed optical librational frequencies:³

$$k_B T_{\text{rot}}^* \simeq \hbar \sum_{\lambda=1}^{N_l} \frac{\omega_\lambda}{2N_l} \coth \left(\frac{\hbar \omega_\lambda}{2k_B T} \right). \quad (10)$$

(c) *Vibrational contribution.* The vibrational contribution, $\langle (E_K^{\text{vib}})_H \rangle$ can be analytically worked out making few assumptions: the displacements, \vec{u}_H , of the protons from their equilibrium positions, \vec{d}_H , are small in comparison with their average distances from the center of mass; the vibrational modes can be dealt within the harmonic approximation and are rather localized and undispersed, so that the optical frequencies (at $q \approx 0$) are comparable with the neutron scattering ones.

Under these assumptions the proton displacements within an isolated water molecule can be decomposed in 3 normal modes, q_λ (symmetric stretching, ν_1 ; bending, ν_2 ; antisymmetric stretching, ν_3), and the \vec{u}_H expressed in terms of the amplitude vectors \vec{C}_H^λ to yield

$$\vec{u}_H = \sum_{\lambda=1}^3 \vec{C}_H^\lambda q_\lambda. \quad (11)$$

Then the proton vibrational mean kinetic energy can be written as

$$\langle (E_K^{\text{vib}})_H \rangle = M_H \sum_{\lambda=1}^3 (\vec{C}_H^\lambda)^2 \frac{\hbar \omega_\lambda}{4} \coth \left(\frac{\hbar \omega_\lambda}{2k_B T} \right), \quad (12)$$

where $\hbar \omega_\lambda$ is now the frequency of the λ th vibrational normal mode.

In summary, the final expression of the temperature dependent mean kinetic energy of a hydrogen atom in liquid H₂O can be written as

TABLE I. Vibrational frequencies of maximum intensity (Raman) for the dense fluid along the coexistence curve and at a supercritical state from Ref. 4. Translational and librational frequencies of maximum intensity (Raman) at the constant pressure of 256 bar³.

Raman frequencies in water (meV)							
T (K)	Stretching modes (ν_1, ν_3)	Bending mode (ν_2)	Translational modes		Librational modes		
303	419.5	201.4	8.2	19.5	52.7	82.5	99.4
423	430.0	201.4	8.3	15.7	30.9	58.4	86.5
513	437.4	201.4	8.6	14.9	30.5	60.1	86.5
603	442.4	201.4	8.3	13.9	31.6	31.7	87.4
663	444.9	201.4	7.9	13.1	30.3	60.5	87.2

$$\begin{aligned} \langle (E_K)_H \rangle &= \langle (E_K^{\text{ext}})_H \rangle + M_H \sum_{\lambda=1}^3 (\vec{C}_H^\lambda)^2 \frac{\hbar \omega_\lambda}{4} \coth \left(\frac{\hbar \omega_\lambda}{2k_B T} \right) \\ &= (0.0839 k_B T_{\text{tra}}^* + 0.71 k_B T_{\text{rot}}^*) \\ &\quad + M_H \sum_{\lambda=1}^3 (\vec{C}_H^\lambda)^2 \frac{\hbar \omega_\lambda}{4} \coth \left(\frac{\hbar \omega_\lambda}{2k_B T} \right). \end{aligned} \quad (13)$$

In Fig. 3 we report the DINS determination of the proton mean kinetic energy in supercritical water (full diamond) together with the calculated values [according to Eq. (13)] for an isolated water molecule (dot–dashed line) and for a dense fluid up to supercritical states (solid circles with the solid line as a guide for the eyes). In order to derive the proton mean kinetic energy in the whole temperature range of interest, the internal vibrational frequencies for the isolated molecule are taken from Ref. 21 and those for the dense fluid along the coexistence curve and at the supercritical state from Ref. 4 (see Table I). In the latter case, bearing in mind the experimental evidence that the external modes have little dependence on the density, values of the roto-translational frequencies have been taken from Ref. 3. The value of the mean kinetic energy calculated from Eq. (13) at the supercritical state is 180.3 meV.

In Ref. 19 it has been shown that the $n_H(\vec{p})$ momentum distribution for a free rotating quasi-symmetrical top molecule, such as for instance H₂S, is better described by an anisotropic Gaussian lineshape and that an analytical determination of $\sigma_{H,\text{cal}}^2(\hat{r})$ can be deduced (see also Ref. 22). Since the mass distribution in a H₂O molecule is less symmetric than in a H₂S molecule, an anisotropic momentum distribution is also expected in the present case. As far as the free rotating molecule approximation is concerned, this represents a fairly good description for supercritical water states, given that the hydrogen bond network is mainly disrupted and only a few dimers are likely to survive.¹ On the contrary we note that in ambient water this approximation could not be invoked. Following the procedure described in Ref. 19, we have calculated, for an isolated water molecule, the semi-classical expression of $\sigma_{H,\text{cal}}^2(\hat{r})$ in the molecular reference frame as

$$\hbar^2 \sigma_{\text{H,cal}}^2(\hat{r}) = \frac{M_{\text{H}}^2}{M_T} k_B T + M_{\text{H}}^2 k_B T \hat{r}^T \mathbf{R}_{\text{H}} \hat{r} + M_{\text{H}}^2 \sum_{\lambda=1}^3 (\vec{C}_{\text{H}}^{\lambda} \cdot \hat{r})^2 \frac{\hbar \omega_{\lambda}}{2} \coth\left(\frac{\hbar \omega_{\lambda}}{2 k_B T}\right), \quad (14)$$

where the tensor \mathbf{R}_{H} is related to the Sachs–Teller mass tensor, \mathbf{S}_{H} , by

$$\mathbf{R}_{\text{H}} = \mathbf{S}_{\text{H}}^{-1} + M_T^{-1} \mathbf{1}, \quad (15)$$

with $\mathbf{1}$ being the unity matrix. The tensor \mathbf{S}_{H} appears in the classical treatment of molecular rotations²³ and depends only on the masses and the intramolecular distances.

We stress that Eq. (14), written for an isolated molecule, can be used in the whole temperature range, up to supercritical dense states. This can be done, as already discussed, by replacing T in the first two terms of Eq. (14) with the effective temperatures T_{tra}^* [see Eq. (8)] and T_{rot}^* [see Eq. (10)], and taking into account the temperature dependence of the internal vibrational frequencies.⁴ Subsequently, as for the H_2S case, $\sigma_{\text{H,cal}}^2(\hat{r})$ can be projected along two symmetry directions of the H_2O molecule: one normal to the molecular plane, \hat{z} , and the other parallel to the molecule plane, \hat{t} . This calculation for $T = 673$ K yields $\sigma_{\text{H,cal}}(\hat{t}) = 3.88 \text{ \AA}^{-1}$ and $\sigma_{\text{H,cal}}(\hat{z}) = 5.99 \text{ \AA}^{-1}$, where the angular average of Eq. (14) provides with the value in the isotropic approximation, namely $\langle \sigma_{\text{H,cal}} \rangle = 5.4 \text{ \AA}^{-1}$. We note the good agreement of this spherical averaged value with the previously reported experimental evaluation (accomplished with the single Gaussian fit).

Given the anisotropic mass distribution in the H_2O molecule, the validity of the above approach can be checked by numerically generating two distinct response functions, obtained from both isotropic and anisotropic momentum distributions, i.e., a Gaussian function with standard deviation $\langle \sigma_{\text{H,cal}} \rangle$ and a multivariate two-dimensional Gaussian function with standard deviations $\sigma_{\text{H,cal}}(\hat{t})$ and $\sigma_{\text{H,cal}}(\hat{z})$, respectively. A fit of the experimental data has been performed by using these two calculated response functions, where standard deviations, in the \hat{t} and \hat{z} directions, have been fixed to the above values, while the intensity factor and the peak centroid have been left free. The fit gives $\bar{\chi}_{\text{aniso}}^2 = 0.54$, to be compared with $\bar{\chi}_{\text{iso}}^2 = 0.55$ for the isotropic approach. This result evidences a full compatibility of the anisotropic momentum distribution model with the experimental data, although the statistical quality of data prevents a clear discrimination between the two models, contrary to the H_2S case.⁵

IV. DISCUSSION AND CONCLUSION

From Fig. 3 we note that the calculated value of the mean kinetic energy for supercritical water appears to be in good agreement with the experimental result. As far as the predicted density and temperature dependence is concerned, differences in the $\langle (E_K)_{\text{H}} \rangle$ values for the isolated molecule and the dense fluid are visible only at temperatures lower than 400 K. Moreover we note that the calculated value of

$\langle (E_K)_{\text{H}} \rangle$ changes, on the average, within a 20 meV window in the whole thermodynamic range considered. A sensible difference between $\langle (E_K)_{\text{H}} \rangle$ values of a proton in an isolated molecule and in the dense fluid was not observed. This can be explained considering that, as the density increases, the intra-molecular stretching modes become softer, while the external modes (mainly hindered rotations and librations) become harder. These two changes seem to compensate each other almost in an exact way.

Present results are in disagreement with both calculated and experimental results reported in Ref. 6. Indeed in that paper a large difference of proton mean kinetic energy values, between diluted gas and dense supercritical water, is predicted (see dot-dashed lines in Fig. 3). This is due to a wrong expression used in Ref. 6 and 24 for the intramolecular contribution to $\langle (E_K)_{\text{H}} \rangle$ of both an isolated molecule and dense fluid. Uffindell *et al.* indeed calculate the proton internal kinetic energy for liquid water at room temperature by means of the following expression,²⁴ where $\langle (E_K^{\text{vib}})_{\text{H}} \rangle$ is wrongly assumed equal to the total energy of a harmonic oscillator:

$$\langle (E_K^{\text{vib}})_{\text{H}} \rangle = \sum_{\lambda=1}^3 \frac{\hbar \omega_{\lambda}}{2} = \frac{200 + 2 \cdot 403}{3 \cdot 2} \text{ meV}. \quad (16)$$

In Eq. (16), 200 meV is the frequency of the bending mode, 403 meV is the equal weight average of the three stretching frequencies³ and the factor 2 accounts for symmetric and antisymmetric stretching modes. The factor 3 assumes equipartition of the kinetic energy among oxygen and hydrogens instead of accounting for the different intensities of the normal modes as done in Eq. (12). An identical incorrect expression is used for the gas state.²⁴

On the experimental side the difference between present result and those reported in Ref. 6 is, in our opinion, to be ascribed to the more accurate cell subtraction procedure employed here (see Sec. II). Indeed we have checked that the analysis of the present set of data with the eVS standard routine provides a value for $\langle (E_K)_{\text{H}} \rangle = (219 \pm 10) \text{ meV}$, which is in agreement with the value, at the same density, reported in Ref. 6. It is reasonable to expect that a bad cell subtraction, which is independent of the thermodynamic state, has affected all data reported in Ref. 6.

We stress that when both cell contribution is reliably subtracted and dependence on the thermodynamic state of internal and external mode frequencies is properly taken into account, the experimental data in the supercritical state are in satisfactory agreement with theoretical predictions. The evolution with the thermodynamic conditions of the hydrogen bond network in water is indeed reflected in the theoretical calculations, through the changes of the vibrational frequencies, and decoupling hypothesis applies as temperature increases.

A last comment regards the use of an anisotropic momentum distribution which, instead of a simple Gaussian distribution was suggested in a previous paper,⁵ to provide a better description of the experimental response function in anisotropic molecular systems. In the present paper, one can

only assess that the anisotropic momentum distribution is compatible with the experimental response function, due to statistical uncertainties of the present data.

In conclusion, data from a DINS measurement on water in the supercritical state have been presented and the mean kinetic energy of the proton inside a H_2O molecule extracted. The experimental response function has also been interpreted taking into account the anisotropic character of the proton momentum distribution in an oriented molecule. It has been found that $\langle(E_K)_H\rangle$ is well described by a semi-classical harmonic model making use of the optical spectroscopic data available in literature. The agreement between the experimental results and the theoretical predictions implies that the hypothesis of both the harmonic approximation and negligible interactions between translational, librational and vibrational degrees of freedom can be reasonably assumed in the supercritical state. In order to assess whether in water the anisotropic momentum distribution model might provide a better description than an isotropic one, higher statistical accuracy of experimental data is required.

ACKNOWLEDGMENTS

The authors gratefully thank Dr. J. Mayers, Dr. A. L. Fielding, and J. Dreyer of the ISIS User Support Group for their kind assistance during the experiment. This work has been partially supported by the *Consiglio Nazionale delle Ricerche* (Italy).

¹P. Postorino, R. H. Tromp, M. A. Ricci, A. K. Soper, and G. W. Neilson, *Nature* (London) **366**, 668 (1993); A. K. Soper, F. Bruni, and M. A. Ricci, *J. Chem. Phys.* **106**, 247 (1997); A. Botti, F. Bruni, M. A. Ricci, and A. K. Soper, *ibid.* **109**, 3180 (1998); T. Tassaing, M.-C. Bellisent-Funel, B. Guillet, and Y. Guissani, *Europhys. Lett.* **42**, 265 (1998).

- ²Y. E. Gorbaty and R. B. Gupta, *Ind. Eng. Chem. Res.* **37**, 3026 (1998).
- ³D. M. Carey and G. M. Korenowski, *J. Chem. Phys.* **108**, 2669 (1998).
- ⁴M. A. Ricci, M. Nardone, A. Fontana, C. Andreani, and W. Hahn, *J. Chem. Phys.* **108**, 450 (1998).
- ⁵C. Andreani, E. Degiorgi, R. Senesi, F. Cilloco, D. Colognesi, J. Mayers, M. Nardone, and E. Pace, *J. Chem. Phys.* **114**, 387 (2001).
- ⁶C. H. Uffindell, A. I. Kolesnikov, J. C. Li, and J. Mayers, *Phys. Rev. B* **62**, 5492 (2000).
- ⁷See Faraday Discussions: "Hydration processes in biological and macromolecular systems," 1996, No. 103, p. 304 (General Discussion).
- ⁸J. Mayers and A. C. Evans, "Measurement of atomic momentum distribution functions by neutron Compton scattering," Rutherford Appleton Laboratory Report No. RAL-91-048, 1991.
- ⁹G. Windsor, *Pulsed Neutron Scattering* (Taylor & Francis, London, 1981).
- ¹⁰R. M. Brugger, A. D. Taylor, C. E. Olson, J. A. Goldstowe, and A. K. Soper, *Nucl. Instrum. Methods Phys. Res. A* **221**, 393 (1984).
- ¹¹C. Andreani, G. Baciocco, R. S. Holt, and J. Mayers, *Nucl. Instrum. Methods Phys. Res. A* **276**, 205 (1991).
- ¹²C. Andreani, D. Colognesi, and E. Pace, *Phys. Rev. B* **60**, 10008 (1999).
- ¹³J. Mayers, "eVs analysis routines for fitting time of flight data," Rutherford Appleton Laboratory Report No. RAL-96-067, 1996.
- ¹⁴A. L. Fielding, J. Mayers, and R. Senesi (unpublished).
- ¹⁵G. I. Watson, *J. Phys.: Condens. Matter* **8**, 5955 (1996).
- ¹⁶W. Lovesey, *Theory of Neutron Scattering from Condensed Matter* (Oxford University Press, Oxford, 1987).
- ¹⁷G. B. West, *Phys. Rev. Lett.* **18**, 263 (1975).
- ¹⁸J. M. F. Gunn, C. Andreani, and J. Mayers, *J. Phys. C* **19**, 835 (1986).
- ¹⁹D. Colognesi, E. Pace, and E. Degiorgi, *Physica B* **293**, 317 (2001).
- ²⁰F. James, *MINUIT Minimization Package: Reference Manual* (CERN Program Library, Geneva, 1994).
- ²¹W. S. Benedict, N. Gailar, and E. K. Plyler, *J. Chem. Phys.* **24**, 1139 (1956).
- ²²G. K. Ivanov, *Sov. Phys. JETP* **17**, 390 (1963); G. K. Ivanov and Yu. S. Sayasov, *Sov. Phys. Usp.* **9**, 670 (1967).
- ²³T. J. Krieger and M. S. Nelkin, *Phys. Rev.* **106**, 90 (1957).
- ²⁴C. H. Uffindell, Ph.D. thesis, University of Manchester—Institute of Science and Technology, 2000.